

ORIGINAL ARTICLE

Normal anatomical and diagnostic imaging techniques of the musculotendinous structures of the ostrich (*Struthio camelus*) foot

Eman A. A. Mahdy¹, Mustafa Abd El Raouf²

¹Department of Anatomy and Embryology, Faculty of Veterinary Medicine, Zagazig University, Zagazig, Egypt

²Department of Surgery, Anesthesiology, and Radiology, Faculty of Veterinary Medicine, Zagazig University, Zagazig, Egypt

ABSTRACT

Objective: The objective of this work was to study the normal musculotendinous structures of the ostrich foot.

Materials and methods: Ten African apparent healthy adult female ostriches (*Struthio camelus*) were slaughtered, and the pelvic limbs were separated from the ankle joint. The different biomedical scanning techniques including radiography, computed tomography (CT), magnetic resonance imaging, and ultrasonography were achieved. Then, the ostrich feet were freshly dissected.

Results: The radiographs and CT images showed the bony components of the ostrich foot that revealed the presence of long tarsometatarsus and phalanges of the only developed third and fourth toes. The third digit was the longest and possessed four phalanges, whereas the shorter fourth toe contained five phalanges. The ostrich foot consisted mainly of tendons in addition to several small associated muscles. The extensor structures were the extensor digitorum longus tendon, Mm. extensor proprius digiti III, and extensor brevis digiti III and IV. On the other hand, the flexor structures were the flexor digitorum longus, flexor hallucis longus, flexor perforans et perforatus digiti III, and flexor perforatus digiti III and IV tendons. Furthermore, fibularis longus tendon and two muscles (Mm. abductor digiti IV and lumbricalis) were related to the flexor tendons.

Conclusion: The combination between the dissecting anatomy and the different biomedical scanning techniques was of value in describing the normal anatomical course of the musculotendinous structures of the ostrich foot, which aids in the diagnosis of any clinical abnormalities in these structures.

ARTICLE HISTORY

Received January 08, 2020

Revised March 10, 2020

Accepted March 17, 2020

Published April 13, 2020

KEYWORDS

Anatomy; computed tomography; magnetic resonance imaging; ostrich foot; radiography; ultrasonography



This is an Open Access article distributed under the terms of the Creative Commons Attribution 4.0 Licence (<http://creativecommons.org/licenses/by/4.0>)

Introduction

The ostrich is believed to be the heaviest and speedy non-flying bird. One stride of the adult ostrich can cover 3.5–7 m, and the speed of the bird reaches up to 50–60 km/h. The ostrich has a great capacity to run 30 min without exhaustion [1]. The running speed is due to the characteristic anatomical structures of the limbs such as strong legs, feet, and coordination between the muscles and tendons [2–4]. The foot is the major actuator in the speedy ostrich strides [1,4], and the tendons achieve an important role in transmitting forces to produce the tarsometatarsus and toe movement. The shapes of the tendon differ from fan, flat, cylindrical, and band shape. These shape variations

are mostly associated to the complex function of the entire musculotendinous system [5,6].

The ostrich tendons are of good quality and suitable length as well as have a similar diameter to humans [7]. Tendon injuries are one of the most common surgical problems in humans [8,9] and equine [10]. The surgical treatment of such conditions requires suturing techniques that should be of high tensile strength and induces a minimal tissue reaction with minimal adhesions [9]. Despite the differences *in vivo* experiments and *ex vivo* biomechanical tests to compare different suture methods, a diversity of repairing techniques is performed clinically, indicating the current nonunified method for the tendon

Correspondence Eman A. A. Mahdy ✉ dr.emanmahdy82@gmail.com 📧 Department of Anatomy and Embryology, Faculty of Veterinary Medicine, Zagazig University, Zagazig, Egypt.

How to cite: Mahdy EAA, Abd El Raouf M. Normal anatomical and diagnostic imaging techniques of the musculotendinous structures of the ostrich (*Struthio camelus*) foot. J Adv Vet Anim Res 2020; 7(2):242–252.

repairing [8]. Hence, the search for new suture styles for tendon reparation using a suitable animal model is motivated. A study was carried out by Karakurum et al. [7] to test the biomechanical properties of ostrich foot tendons and explained their importance in the analysis of the recently designed suture methods for hand surgery in human. Therefore, detailed information about the musculotendinous structures of the ostrich pelvic limb is needed. The morphology of the musculoskeletal system of the ostrich limb has been demonstrated in several previous studies [11–15] but restricted to describe the muscles of the ostrich limb and modernize its nomenclatures. Furthermore, the recent ostrich locomotion investigations gave attention to the structure, kinematics, and dynamics of the ostrich limb [16–18]. Despite all these studies, there are lacked details about the morphology and biomedical scanning of the tendons of the leg and the foot locomotion system of the ostrich. Hence, the objective of the current work was to study the normal musculotendinous structures of the ostrich foot using different biomedical scanning techniques including radiography, computed tomography (CT), magnetic resonance imaging (MRI), and ultrasonography combined with dissecting anatomy and provides information to help in the diagnosis of clinical abnormalities in these structures in ostriches.

Materials and Methods

Ethical statement

All the practices in this work were conducted according to animal use rules and care of Zagazig University (ZU-IACUC/2/F/4/2020), Egypt.

Birds

For studying the musculotendinous structures of the ostrich foot, 10 African apparent healthy adult female ostriches (*Struthio camelus*) in Gamal's Ostrich Farm, Belbeis, Egypt, were slaughtered, and the pelvic limbs ($n = 20$) were separated from the intertarsal (ankle) joint.

Biomedical scanning techniques

The ostrich feet were used for radiographic examination by X-ray device (Pox-300 BT, Toshiba, Rotanode™, Japan) using 45 kV and 6.3 mAs, CT scans (Hitachi, USA, Multislice 16 scanner) with 120 kV and 200 mA, MRI scanning (Siemens, 1.5T MRI scanner, USA), and ultrasonographic examination using an ultrasound machine (Esaote MyLab One, Italy) connected with 6-MHz linear transducer and 7 cm depth. In the ultrasonographic examination, the tarsometatarsal region was divided into six-zone areas; each was 7 cm in length for demonstrating the extensor and flexor structures at the dorsal and plantar aspects of the tarsometatarsus, respectively.

Anatomical procedures

The ostrich feet were freshly dissected and photographed with a high-resolution digital camera (32 megapixels, Sony DSC-W690). Then, the feet were immersed in a fixative solution (10% formalin, 3% glycerine, and 1% thymol). Subsequently, measurements of the thickness and width of both extensor and flexor tendons were performed using a caliper. The measurement data were statistically analyzed using SPSS software (version 17, Chicago, IL). The nomenclature of the structures was used following the previously described [14,19].

Results

The only developed toes in the ostrich were the third and fourth ones. The third digit appeared the longest and possessed four phalanges, whereas the shorter fourth toe contained five phalanges as appeared in radiographs and CT images (Fig. 1A–D). The muscles and tendons exhibited in the ostrich foot inserted mainly in the tarsometatarsus and the phalanges of the toes (Figs. 1E and F, 2, 3 and 4). The musculotendinous structures on the dorsal and plantar sides of foot were demonstrated anatomically and scanned with different biomedical techniques as follows:

Extensor digitorum longus tendon

The extensor digitorum longus tendon was the largest and longest extensor tendon in the ostrich foot. Proximally at the tarsometatarsus, this tendon was located medial to the tendon of M. tibialis cranialis and M. extensor proprius digiti III. There were Retinaculum extensorium tarsometatarsi followed by a fascial wrapping sheet distally to retain the tendon of M. extensor digitorum longus. The extensor digitorum longus tendon together with extensor proprius digiti III muscle ran distally in Sulcus extensorius tarsometatarsi (Fig. 1E and F). The tendon was three-sided and narrow proximally but flattened and wide distally (Table 1). Proximal to the metatarsophalangeal joints, the extensor digitorum longus tendon was divided into two Crura such as laterale and mediale. These Crura fixed to the latter joints of the two digits by a strong fascia. Dorsal to Incisura intertrochlearis of the tarsometatarsus, Crus laterale split into Tendo lateralis and Tendo medialis. Tendo lateralis attained the fourth toe to end on the extensor tubercle of the fifth phalanx, and also a few fibers inserted into the fourth phalanx. Additional divisions were detached laterally and medially from Tendo lateralis to the plantar ligament of the first interphalangeal articulation. Tendo medialis of Crus laterale accompanied the extensor proprius digiti III tendon to the third toe. The two tendons decreased in its thickness distally and became wider. The extensor digitorum longus tendon ended deep to the extensor proprius digiti III tendon in the extensor

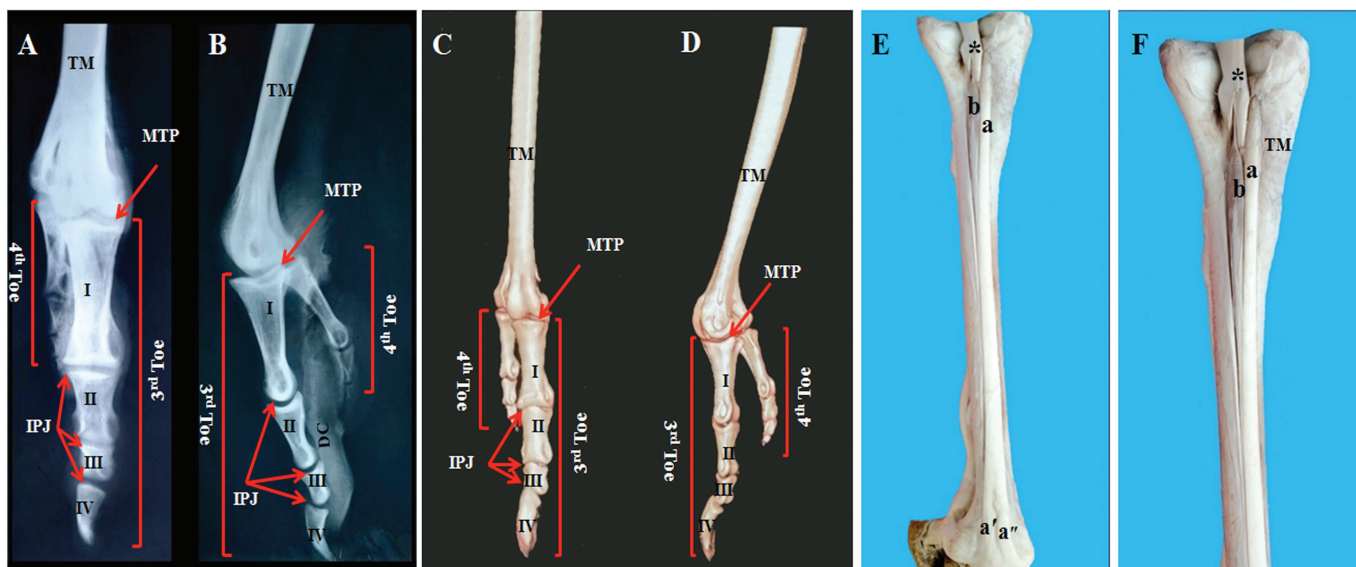


Figure 1. Radiography and CT (three-dimensional image) of the ostrich foot. (A and C) Dorsoplantar view and (B and D) Mediolateral view. MTP- Metatarsophalangeal joint; IPJ: Interphalangeal joints; TM: Tarsometatarsal bone; DC: Digital cushion; I—First phalanx; II—Second phalanx; III- —Third phalanx; IV—Fourth phalanx. Dorsal view of the ostrich foot (E) and (F higher magnification) showing; a—Extensor digitorum longus tendon; a'—Its Crus laterale; a"—Its Crus mediale; b—M. extensor proprius digiti III; asterisk (*)—Tibialis cranialis tendon; TM—Tarsometatarsal bone.

Table 1. Measurements of the extensor and flexor tendons in the tarsometatarsal region of ostrich (the mean \pm standard deviation (SD)).

Tendon	Proximal part		Middle part		Distal part	
	Thickness (mm)	Width (mm)	Thickness (mm)	Width (mm)	Thickness (mm)	Width (mm)
Extensors						
Tendon of M. extensor digitorum longus	5.04 \pm 0.13	7.98 \pm 0.11	3.99 \pm 0.12	9.99 \pm 0.12	3 \pm 0.12	14.95 \pm 0.14
Tendon of M. extensor proprius digiti III	Muscle 12 cm in length 11.96 \pm 0.14		1.44 \pm 0.1	2.43 \pm 0.11	0.95 \pm 0.11	1.9 \pm 0.13
Tendon lateralis of M. fibularis longus	3.01 \pm 0.12	5.97 \pm 0.09	Fused with Tendon of M. flexor perforatus digiti III			
Tendon of M. flexor perforatus digiti IV	7 \pm 0.12	5.03 \pm 0.13	5.03 \pm 0.13	7.98 \pm 0.11	9.97 \pm 0.09	9.97 \pm 0.09
Flexors						
Tendon of M. flexor perforatus digiti III	7.96 \pm 0.08	15.98 \pm 0.11	6.99 \pm 0.12	14.96 \pm 0.13	5.96 \pm 0.1	18.97 \pm 0.13
Tendon of M. flexor perforans et perforatus digiti III	3.01 \pm 0.1	8.45 \pm 0.08	3.97 \pm 0.09	7.48 \pm 0.09	9.98 \pm 0.11	9.98 \pm 0.11
Tendon of M. flexor hallucis longus	9.99 \pm 0.12	7.97 \pm 0.12	5.96 \pm 0.08	7.99 \pm 0.11	Fused with Tendon of M. flexor digitorum longus	
Tendon of M. flexor digitorum longus	2.99 \pm 0.12	6.98 \pm 0.09	5.03 \pm 0.13	4 \pm 0.12	7.46 \pm 0.08	11.47 \pm 0.12

tubercle of the third phalanx. Furthermore, the lateral and medial divisions were given off from the former tendon to attach in the plantar ligament of the middle interphalangeal joint. On the other hand, the medial Crus of the extensor digitorum longus tendon attained the third digit and was separated into two branches such as superficial and profound. The superficial branch was inserted medially in the plantar ligament of the proximal interphalangeal articulation. The profound branch had two insertions; a shorter part inserted laterally in the plantar ligament of the proximal interphalangeal articulation, whereas its

longer attachment terminated on the extensor tubercle of the second phalanx (Fig. 2A and B).

M. extensor proprius digiti III

On the proximal third of the tarsometatarsus, M. extensor proprius digiti III located lateral to the tendon of M. extensor digitorum longus. This muscle composed of a small muscular part (12 cm) and a longer thread-like tendon. The extensor proprius digiti III muscle originated by a small tendon, which appeared between the bifurcated end tendon of M. tibialis cranialis. Above the middle of

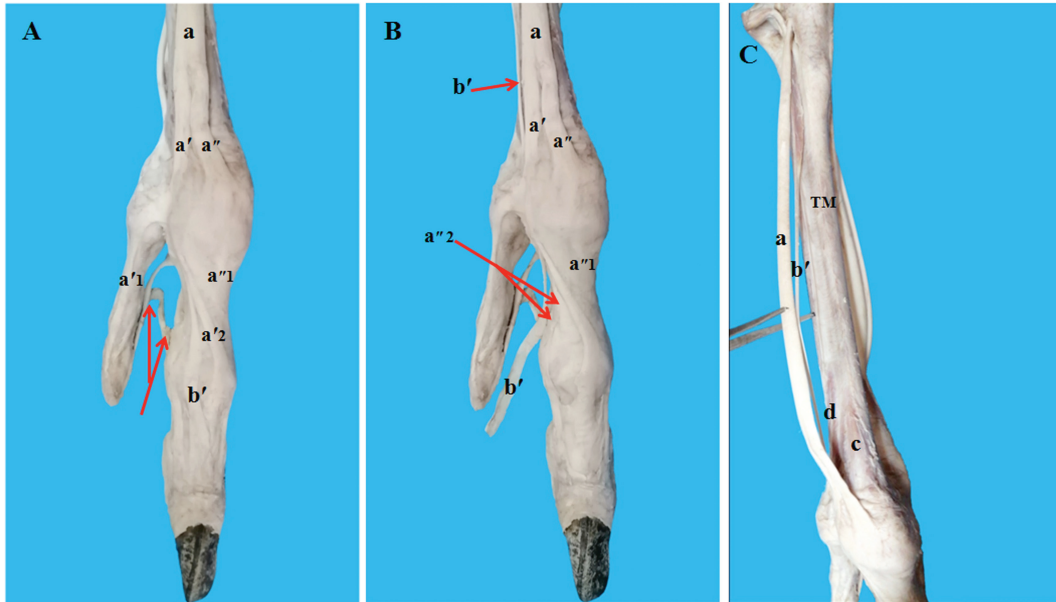


Figure 2. Dorsal view of the digits (A and B) and foot (C) of ostrich showing; a—Extensor digitorum longus tendon; a'—Its Crus laterale; a'1—Tendo lateralis of the Crus lateralis; a'2—Tendo medialis of the Crus lateralis; a''—Crus mediale; a''1—Its superficial part; a''2—Its Deep part; b'—extensor proprius digiti III tendon; Interdigital ligaments (arrows); c—M. extensor brevis digiti III; d—M. extensor brevis digiti IV; TM—Tarsometatarsal bone.

tarsometatarsus, this muscle converted to a very small tendon, which lay plantolaterally of the extensor digitorum longus tendon (Fig. 1E and F). Passing over the first phalanx of the third digit, the tendon became wider, flattened, and appeared lateral to the extensor digitorum longus tendon (Tendo medialis of Crus laterale of the extensor digitorum longus tendon). Then, the extensor proprius digiti III tendon passed dorsal to the tendon of M. extensor digitorum longus to terminate on the extensor tubercle of the terminal phalanx of the third toe (Fig. 2A and B).

M. extensor brevis digiti III

The extensor brevis digiti III muscle was dorsally located on the distal third of tarsometatarsus and medial to extensor brevis digiti IV muscle. It was slightly wider and shorter than the latter muscle. It passed dorsal to the metatarsophalangeal joint to end on basis of the first phalanx of the third toe (Fig. 2C).

M. extensor brevis digiti IV

The extensor brevis digiti IV muscle was narrower and longer and originated from the tarsometatarsus proximolateral to the extensor brevis digiti III muscle. It passed through Incisura intertrochlearis to terminate medially in the base of the proximal phalanx of the fourth toe (Fig. 2C).

Fibularis longus tendon

Tendo lateralis of M. fibularis longus was a small zig-zag-like tendon and not so hard in texture. It lay laterally

within the Vagina fibrosa and joined the flexor perforatus digiti III tendon at the beginning of the middle third of tarsometatarsus (Fig. 3A).

Flexor perforans et perforatus digiti III tendon

The flexor perforans et perforatus digiti III tendon was the most superficial plantar tendon under the skin (Fig. 3A–C). It lay in a groove on the plantar face of the flexor perforatus digiti III tendon. In the distal third of the tarsometatarsus, the flexor perforans et perforatus digiti III tendon joined with that of M. flexor perforatus digiti III via a tendinum Vinculum. The previously mentioned tendons in addition to the flexor perforatus digiti IV tendon were flattened proximally and three-sided distally near the metatarsophalangeal joint. At the latter joint, the tendon of M. flexor perforans et perforatus digiti III coursed deep to the flexor perforatus digiti III tendon in a longitudinal furrow in the plantar ligament of the third digit. All the flexor tendons were enclosed in Vagina fibrosa flexoria. Furthermore, there were four strong plantar fascial pulleys covering the flexor tendons at the interphalangeal joints of the two digits (Fig. 4A). At the level of the first phalanx of the third toe, the flexor perforans et perforatus digiti III tendon appeared superficial again between the divergent tendon of insertion of M. flexor perforatus digiti III. It was flattened and branched into two Crura which terminated medially and laterally in the plantar ligament of the middle interphalangeal articulation (Fig. 4B).

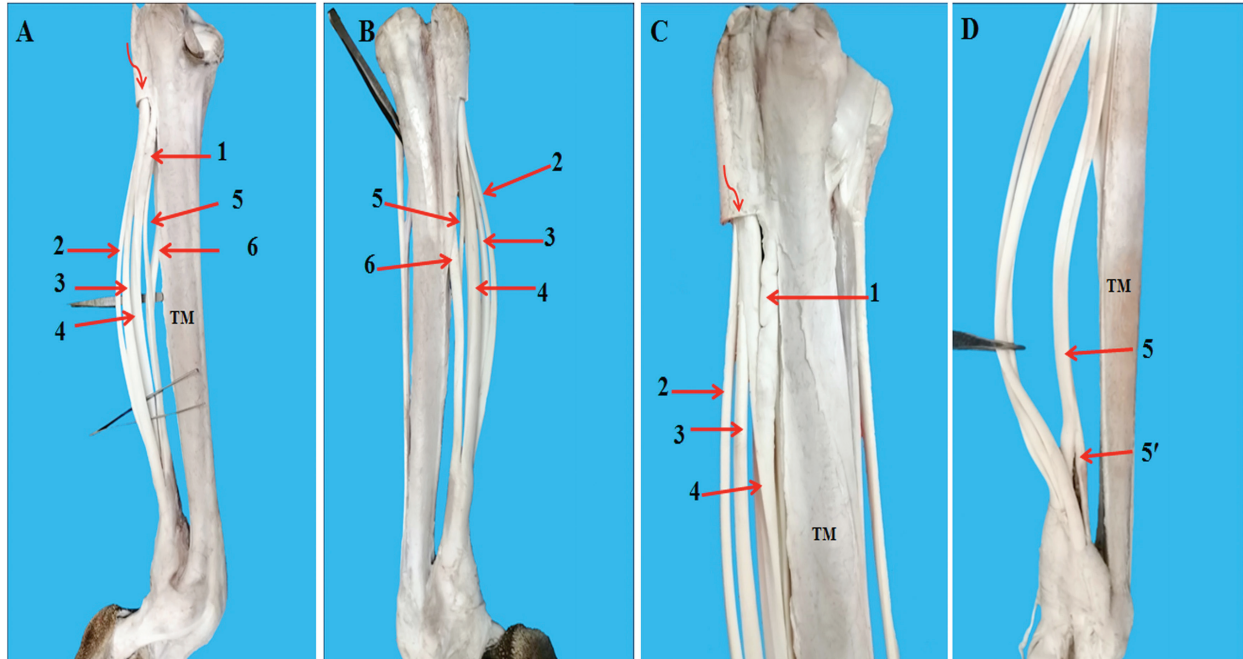


Figure 3. The flexor tendons of the ostrich foot lateral view (A, C, and D) and medial view (B) showing; 1—Tendo lateralis of *M. fibularis longus*; 2—Fexor perforans et perforatus digiti III tendon; 3—Fexor perforatus digiti IV tendon; 4—fexor perforatus digiti III tendon; 5—fexor digitorum longus tendon; 5'—A small tendon for the 4th toe; 6- Fexor hallucis longus tendon; Vagina fibrosa flexoria (cut) (curved arrow); TM—Tarsometatarsal bone.

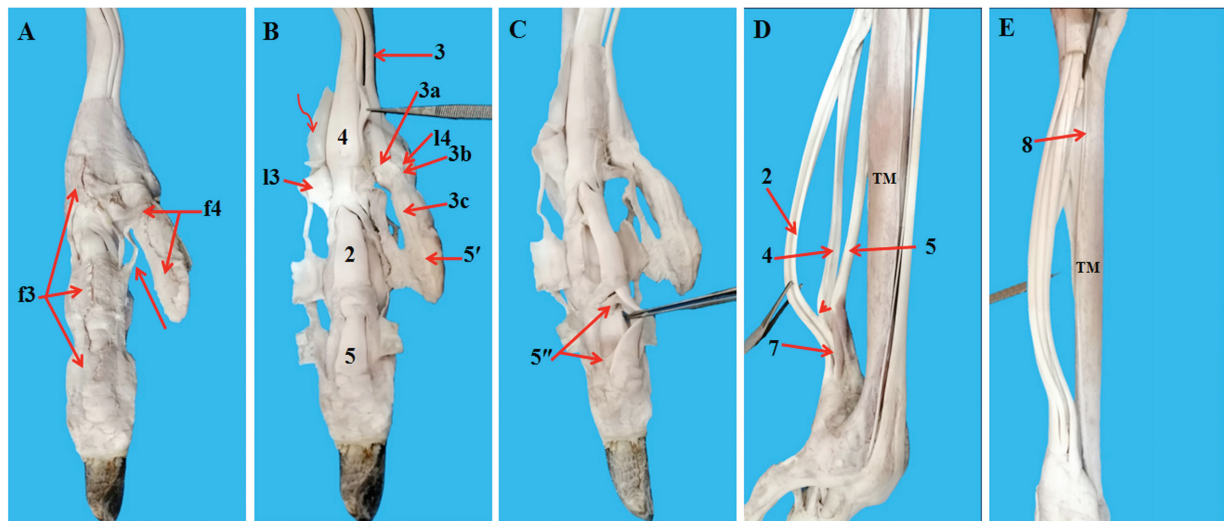


Figure 4. Plantar view of the digits (A, B and C) and lateral view of the foot (D and E) of ostrich showing; f3- Fascia casing (pulleys) the interphalangeal joints of the 3rd toe and 4th toe (f4); Interdigital ligament (arrow); Vagina fibrosa flexoria (reflected) (curved arrow); l3—Annular ligament (cut) of the 3rd toe and of the 4th toe (l4); 2—Fexor perforans et perforatus digiti III tendon; 3—Fexor perforatus digiti IV tendon; 3a—Its Crus proximale; 3b—Its Crus intermedium; 3c—Its Crus distal; 4—fexor perforatus digiti III tendon; 5—fexor digitorum longus tendon; 5'—A small tendon for the 4th toe; 5''—Ligamenta elastica tendinis flexoris ; 7—*M. lumbricalis*; 8— *M. abductor digiti IV*; TM—Tarsometatarsal bone; Vinculum tendinum flexorum connected the tendons of *Mm. fexor perforans et perforatus digiti III* and *fexor perforates digiti III* (arrow head).

Flexor perforatus digiti III tendon

The tendon of *M. flexor perforatus digiti III* was the largest flexor tendon in the tarsometatarsus. Proximally, it encircled the flexor perforatus digiti IV tendon and showed a plantar longitudinal groove for the flexor perforans et perforatus digiti III tendon (Fig. 3A–C). Subsequently, this tendon lay dorsally and had two plantar longitudinal grooves for the previous two mentioned tendons. At the middle third of tarsometatarsus, fibularis longus tendon united with that of flexor perforatus digiti III muscle, and the latter became medial to the flexor perforans et perforatus digiti III and flexor perforatus digiti IV tendons. Proximal to the metatarsophalangeal joints, the flexor perforatus digiti III tendon was located plantar to the abovementioned tendons. It lay in a groove on the plantar ligament of the metatarsophalangeal joint, and distally, the flexor perforatus digiti III, flexor perforans et perforatus digiti III, and flexor digitorum longus tendons were maintained with an annular ligament. Just below to the latter ligament, the flexor perforatus digiti III tendon ended by splitting up into two Crura which inserted laterally and medially on the distal extremity of the first phalanx and in the plantar ligament of the first interphalangeal articulation of the third toe (Fig. 4B).

Flexor perforatus digiti IV tendon

The tendon of *M. flexor perforatus digiti IV* was entirely enclosed by the flexor perforatus digiti III tendon at the proximal portion of tarsometatarsus (Fig. 3A–C). After that, it exposed on a longitudinal groove on the plantar face of the same tendon. Plantarily on the metatarsophalangeal joint of the fourth phalanx, the flexor perforatus digiti IV and flexor digitorum longus tendons were surrounded by an annular ligament. The aforementioned tendon as was divided into three parts; Crus proximale was the shortest and attached medially at the base of the first phalanx. Crus intermedium inserted in the plantar ligament of the first interphalangeal joint. Meanwhile, Crus distale was the longest and ended in the plantar ligament of the middle interphalangeal articulation (Fig. 4B).

Flexor hallucis longus tendon

The tendon of *M. flexor hallucis longus* was separated alone in a synovial sheath in the proximal third of the tarsometatarsus. After about 15.5 cm, it exited and passed on a groove in the dorsal face of the flexor perforatus digiti III tendon. As soon as at the mid tarsometatarsus, this tendon merged with that of flexor digitorum longus muscle (Fig. 3A and B).

Flexor digitorum longus tendon

The flexor digitorum longus tendon ran laterally on the plantar face of tarsometatarsus and dorsal to the tendon

of *M. flexor perforatus digiti III*. Almost on the distal half of tarsometatarsus, this tendon retained by its combination with the tendon of flexor hallucis longus muscle (Fig. 3A). Close to lumbricalis muscle, the tendon gave off a small lateral branch for the fourth digit (Fig. 3D). The splitting tendon passed distally plantolateral to *M. lumbricalis* in a longitudinal furrow on the dorsal surface of flexor perforatus digiti IV tendon. It lay on the plantar ligament of the metatarsophalangeal joint and appeared again among the intermediate and distal insertions of flexor perforatus digiti IV muscle. The tendon coursed lateral to the distal end tendon of flexor perforatus digiti IV muscle and inserted in the flexor tubercle of the distal phalanx of the fourth toe. The chief flexor digitorum longus tendon attained the third toe deep to the flexor perforatus digiti III and flexor perforans et perforatus digiti III tendons. Finally, it became superficial distal to the insertion of the latter muscle and terminated in the flexor tubercle of the terminal phalanx of the digit (Fig. 4B). The flexor digitorum longus tendon provided dorsally a three Ligamenta elastica tendinis flexoris to the plantar ligament of the interphalangeal joints (Fig. 4C).

M. lumbricalis

M. lumbricalis was situated dorsally on the flexor digitorum longus tendon on the distal third of tarsometatarsus. Lumbricalis muscle splits into two parts to be inserted on the plantar face of metatarsophalangeal joints of the two digits of ostrich (Fig. 4D).

M. abductor digiti IV

Abductor digiti IV muscle was a small musculotendinous, resting along the plantar face of tarsometatarsus and dorsal to the flexor group of tendons. Below the middle of tarsometatarsus, the muscle ran laterally to Vagina fibrosa flexoria. Just above the metatarsophalangeal joint, the tendon passed in a fibrocartilaginous groove and restrained by a Retinaculum. It terminated just distal to the base of the proximal phalanx of the fourth toe (Fig. 4E).

Radiographic and CT findings

Radiographs (dorsoplantar and mediolateral views) and CT (sagittal and three dimensional) imaging of the ostrich foot revealed radiopaque tarsometatarsal and phalangeal bones of the third and fourth toes. The metatarsophalangeal joint was formed by the articulation between the tarsometatarsus and the first phalanx of the third and fourth toes. Interphalangeal joints were formed by the articulation between the phalangeal bones. The digital cushion of the foot appeared radiographically as a radiopaque structure at the plantar aspect of the third toe (Fig. 1A–D). In the coronal images of CT scanning, the tendons at the dorsal and plantar aspects of the foot appeared as faint radiodense

structures. The anatomical course of the extensor and flexor tendons could be determined at different areas of the limb as described in dissecting anatomy (Fig. 5A).

MRI findings

The MRI scanning of the ostrich foot revealed the anatomical course of the extensor and flexor tendons as described in dissecting anatomy. They appeared as radiolucent structures (Tesla 1 scanning) at the dorsal and plantar aspects of the bones (Fig. 5B). Digital cushions appeared as radiodense structures under the phalanges.

Ultrasonographic findings

Dorsal aspect of tarsometatarsus

The ultrasonographic examination of each area of the extensor structures at the dorsal aspect of the tarsometatarsus revealed as follows: **At zone 1:** the presence of echogenic structure represents the end tendon of tibialis

cranialis muscle and origin of extensor proprius digiti III muscle that seemed a hypoechogenic structure underneath the skin. The echogenic structure with parallel oriented fibers represents the extensor digitorum longus tendon (Fig. 6E1). **At zone 2:** the bulk of M. extensor proprius digiti III appeared as a hypoechogenic mass with the starting of its tendinous part that appeared as an echogenic structure with oriented fibers under the skin and the extensor digitorum longus tendon (Fig. 6E2). **At zone 3:** the well-oriented echogenic fibers of the tendon of M. extensor digitorum longus appeared under the skin, and the end of the extensor proprius digiti III muscle appeared as a hypoechogenic structure with echogenic structure of its tendon under the extensor digitorum longus tendon (Fig. 6E3). **At zone 4 and 5:** the extensor digitorum longus and extensor proprius digiti III tendons appeared under the skin (Fig. 6E4 and E5). **At zone 5:** the extensor digitorum longus tendon was divided into two equal parts in addition to the tendon of M. extensor proprius digiti

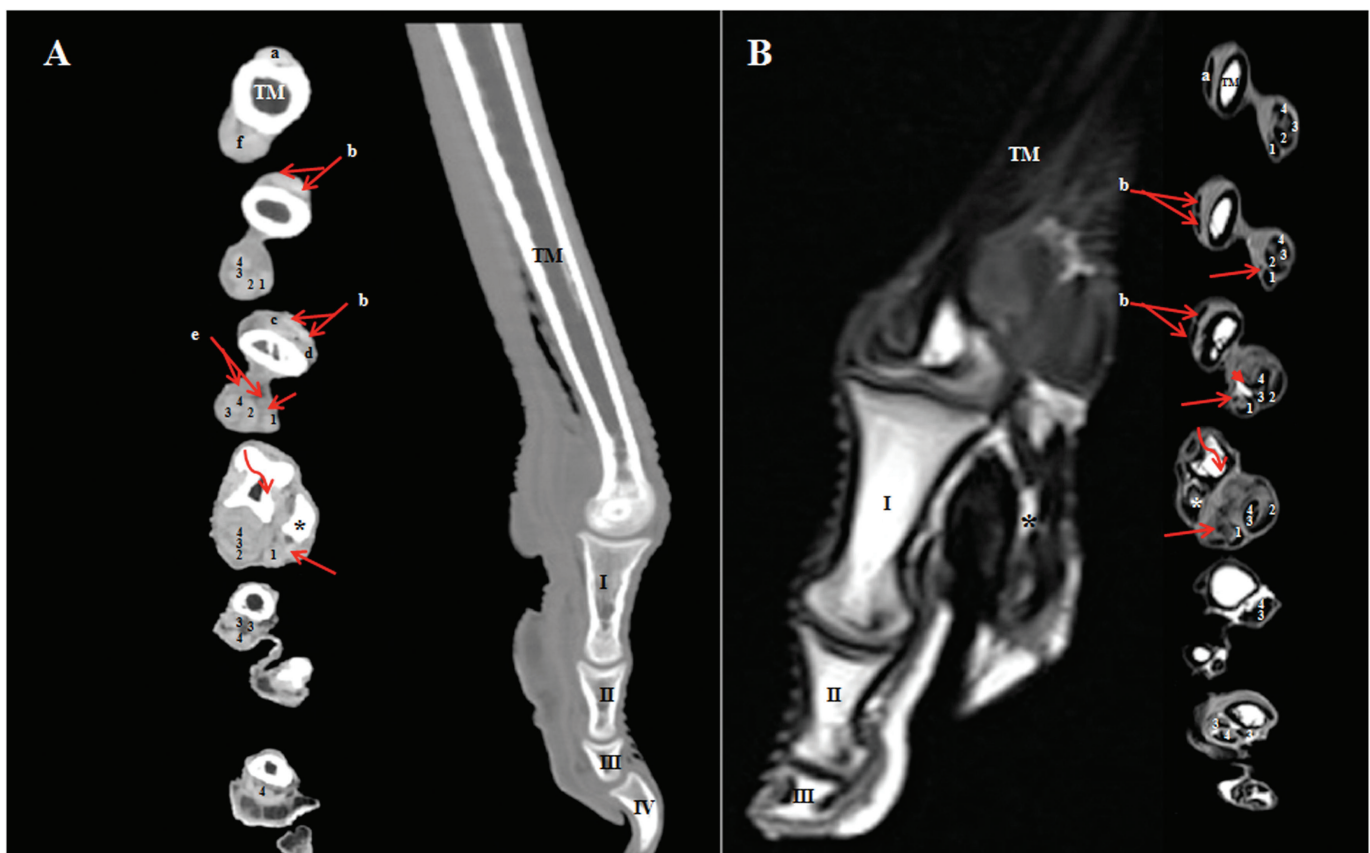


Figure 5. CT, coronal and Sagittal scanning, (A) and MRI, longitudinal and transverse scanning, (B) of the ostrich foot. TM—Tarsometatarsal bone; I—First phalanx; II—Second phalanx; III—Third phalanx; IV—Fourth phalanx; a—extensor digitorum longus tendon; b—lateral and medial branches of extensor digitorum longus tendon; c—M. extensor brevis digiti III; d—M. extensor brevis digiti IV; e—M. lumbricalis; f—the flexor tendons; 1—flexor perforatus digiti IV tendon; 2—flexor perforatus digiti III tendon; 3—flexor perforans et perforates digiti III tendon; 4—flexor digitorum longus tendon. Note the lateral branch of the flexor digitorum longus tendon (arrow), fibrocartilage (arrow head), the third digit (curved arrow) and the fourth digit (asterisk).

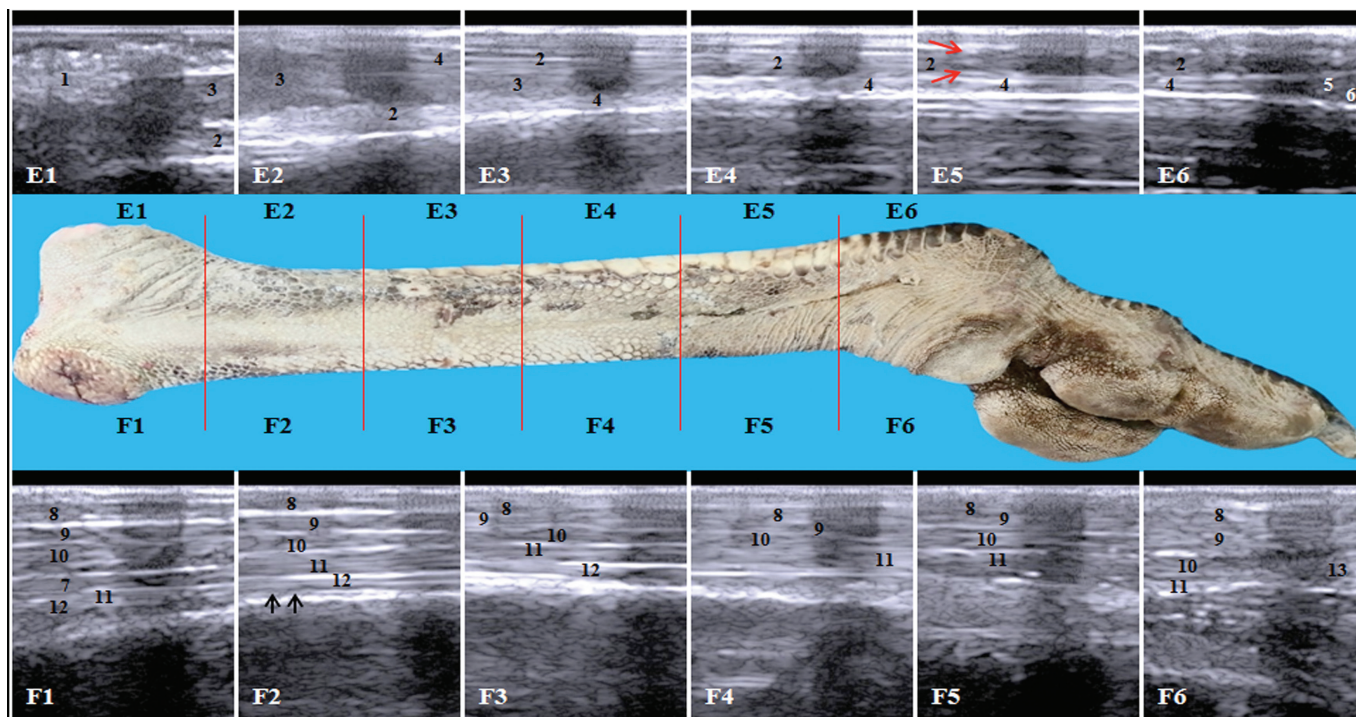


Figure 6. Ultrasonographic imaging of the dorsal aspect (E1–E6) and the plantar aspect (F1–F6) of the tarsometatarsal region of the ostrich. 1—tibialis cranialis tendon; 2—extensor digitorum longus tendon; 3—M. extensor proprius digiti III; 4—extensor proprius digiti III tendon; 5—M. extensor brevis digiti III; 6—M. extensor brevis digiti IV; 7—Tendo lateralis of M. fibularis longus; 8—flexor perforans et perforates digiti III tendon; 9—M. flexor perforatus digiti IV tendon; 10—flexor perforatus digiti III tendon; 11—flexor digitorum longus tendon; 12—flexor hallucis tendon; 13—M. lumbricalis. Note the bifurcation of the extensor digitorum longus tendon (red arrows) and M. abductor digiti IV (black arrows).

III (Fig.6E5). **At zone 6:** the presence of hypoechoic muscular structures of Mm. extensor brevis digiti III and IV, respectively under the extensor digitorum longus and extensor proprius digiti III tendons (Fig. 6E6).

Plantar aspect of tarsometatarsus

Ultrasonographic examination of each area of the flexor structures at the plantar aspect of the tarsometatarsus revealed as follows: **At zone 1:** the presence of echogenic tendinous structures represents the flexor perforans et perforates digiti III, flexor perforates digiti III and IV, flexor digitorum longus, flexor hallucis longus tendons, and lateral tendon of fibularis longus muscle that joined to the tendon of M. flexor perforates digiti III (Fig.6F1). **At zone 2:** echogenic tendinous structures of flexor perforans et perforates digiti III, flexor perforates digiti III and IV, flexor digitorum longus, and flexor hallucis longus muscles appeared in addition to M. abductor digiti IV that appeared as small flattened hypoechoic structure under the tendons (Fig. 6F2). **At zone 3:** echogenic tendinous structures of flexor perforans et perforates digiti III, flexor perforates digiti III and IV, flexor digitorum longus, and flexor hallucis longus muscles appeared (Fig. 6F3).

At zone 4: flexor digitorum longus and flexor hallucis longus tendons joined together and continued distally as flexor digitorum longus tendon in addition to the flexor perforans et perforates digiti III and flexor perforates digiti III and IV tendons (Fig. 6F4). **At zone 5:** the presence of the flexor perforans et perforates digiti III, flexor perforates digiti III and IV, and flexor digitorum longus tendons (Fig. 6F5). **At zone 6:** the presence of hypoechoic muscular structure of M. lumbricalis attached to the flexor digitorum longus tendon in addition to the flexor perforans et perforates digiti III, and flexor perforates digiti III and IV tendons (Fig. 6F6).

Discussion

The locomotor system of the ostrich foot had the attraction of researchers in the past decade as the ostrich is considered the strongest and the fastest among bird populations [16–18]. The importance of studying the ostrich locomotor system is to provide detailed information about the musculotendinous structures of the ostrich foot that will be helpful for human and veterinary surgeries for introducing newly designed suture techniques suitable for tendon

repair. As the previous studies lacked detailed data about the dissecting anatomy and biomedical scanning of the tendinous structures of the foot, therefore, the present study was considered to be the first to provide detailed information about biomedical scanning of the foot of ostrich using radiography, CT, MRI, and ultrasonography.

In this study, the radiographs and CT images showed structural anatomy of the ostrich foot, which revealed the presence of the third and fourth toes with four and five phalanges, respectively. Similar findings were reported by Gangl et al. [14]. However, Karakurum et al. [7] recorded the presence of four phalanges at the fourth toe. Besides, the same authors recorded that the flexor tendons were three in the third digit and two in the fourth digit, which was corresponding to the findings.

Functionally, the muscular and tendinous structures of the ostrich pelvic limb are responsible for bipedal locomotor activity and energy cost [20]. *M. extensor digitorum longus* inserted by two tendons, which assured the previous findings of Gangl et al. [14] and Liswaniso [21]. While the descriptions of Karakurum et al. [7] about the flexor tendons of the third toe were rather the same as of Gangl et al. [14] and the present study, the flexor tendons of the fourth digit were different to some extent. The former authors described an inverse to the result, the tendon of *M. flexor perforatus digiti IV* inserted by the lateral and medial branches which terminated in the bases of the second and third phalanges, respectively. According to Liswaniso [21], the flexor digitorum longus tendon sent a fibroelastic structure to the plantar ligament of the middle interphalangeal articulation of the third digit, the structure which resembled *Ligamentum elasticum tendinis flexoris* [22]. Furthermore, the result and Gangl et al. [14] recorded that these ligaments were three in number connecting the tendon of *M. flexor digitorum longus* to the interphalangeal joints of the third toe. Furthermore, Liswaniso [21] revealed the presence of many muscular insertions on the plantar ligaments of the interphalangeal joints.

The findings described the insertion of *M. abductor digiti IV* in the base of proximal phalanx of the fourth digit, which resembles the previous investigations of Bezuidenhout [11], Gangl et al. [14], and Pavaux and Lignereux [23]. Only Gangl et al. [14] mentioned that the tendon ran in a fibrocartilaginous groove and restrained by a *Retinaculum*, which confirmed by the MRI scanning in the present study. The flexor digitorum longus tendon ran over the whole length of the third digit to end in the fourth phalanx, and thus, it was likely to be affected by the movement of each phalanx. The tendon of *M. flexor perforans et perforatus digiti III* was inserted by two branches in the second phalanx. Hence, the majority of the flexor motion of the third digit controlled by the flexor perforans et perforatus digiti III tendon, whereas the two end branches

of flexor perforatus digiti III tendon attached to the first phalanx [24]. These findings proved to be accurate in the current study.

Flexor perforatus digiti III muscle considered as extensor to the intertarsal joint and flexor to the third digit [20]. Its tendon combined with the lateral tendon of *M. fibularis longus* on the upper part of the tarsometatarsus [14]. The flexor tendon and its sheath have a close relationship in maintaining the tarsometatarsophalangeal joint elevated above the land [4]. After Karakurum et al. [10], four strong plantar pulleys encircled the flexor tendons. These pulleys located at the base of the proximal phalanx, the first and third interphalangeal joints, and alongside the third phalanx. These findings were in agreement with the investigation.

All the flexor digital tendons were slender and long. The flexor perforans and perforatus digiti III tendon was long (990 mm) but had a small cross-sectional area (0.4 cm²), whereas the flexor perforatus digiti III tendon was short in length (680 mm) and large in its cross-sectional zone (1.5 cm²). The greater cross-sectional zone of the latter tendon allowed it to envelop and enclose the smaller flexor perforans and perforatus digiti III and flexor perforatus digiti IV tendons. The flexor digitorum longus tendon was deeply located and measured 900 mm in length and 0.7 cm² in cross-sectional area and received the flexor hallucis longus tendon on the mid tarsometatarsus [25]. The thickness and width of these tendons measured in our result confirmed this finding.

Ultrasonography was considered a rapid, non-invasive, frugal and easily used biomedical method for musculoskeletal system of animals. It could be applied directly to the skin without harmful effects to the animal just using coupling gel to overcome air artifacts [26]. Ultrasonography of the dorsal and plantar aspects of the tarsometatarsal region revealed the presence of tendinous structures with characteristic tendon fiber orientation. The extensor tendons could be identified easily in the dorsal aspect. On the other hand, the tendons of the plantar aspect were hardly distinguished from each other due to their enclosing in *Vagina fibrosa flexoria* and appeared as one bundle. The ultrasonographic findings were in correspondence with the dissecting anatomy in the same areas. The ultrasonography of the digital structures was very difficult due to the presence of thick horny scales on the ostrich skin at this area on the dorsal aspect and presence of the thick digital cushion on the plantar side.

The use of MRI in describing the tendinous structures in the foot region is very important to demonstrate the anatomical course of each tendon [16]. Sagittal and coronal scanning revealed the same course of the tendons on the dorsal and plantar aspects as described in dissecting anatomy.

However, several limitations are worth noting. The presence of thick horny scales and digital cushion at the dorsal and plantar aspects of the digit, respectively, interferes with ultrasonography of this region. Besides, the enclosing of all the flexor tendons in Vagina fibrosa flexoria at the plantar aspect of the tarsometatarsus leads to difficulty distinguishing between them.

Conclusion

The combination between the dissecting anatomy and the different biomedical scanning techniques was of value in describing the normal anatomical course of the musculotendinous structures of the ostrich foot, which assist in the diagnosis of clinical abnormalities in these structures. Ultrasonography was an easy, economic, and non-invasive diagnostic technique and could be used for the diagnosis of tendon injuries in these areas. Further studies needed to determine the value of ostrich tendons in testing newly designed suture techniques for tendon repair.

Acknowledgment

We are grateful to all staff members of Anatomy and Embryology and Surgery, Anesthesiology and Radiology Departments, Faculty of Veterinary Medicine, Zagazig University, Egypt, for the supportive care during the work. Moreover, we awarded great gratitude to Mohammed El-Shafei, Agricultural engineer in Gamal's Farm for Ostriches, Belbeis, Egypt, for his good cooperation with us and providing us with specimens.

Conflict of interest

The authors state that they have no competing interests.

Authors' contribution

Dr. Eman Abd El-Rahman Ahmed Mahdy collected the specimens and performed all the anatomical procedures. Dr. Mustafa Abd El Raouf was responsible for different biomedical scanning techniques. All authors obtained the data, wrote the article, reviewed and formatted data, and approved the manuscript.

References

- [1] Zhang R, Liu HB, Zhang SH, Zeng GY, Li JQ. Finite element analysis in the characteristics of ostrich foot toenail traveling on sand. *Appl Mech Mater* 2013; 461:213–9; <https://doi.org/10.4028/www.scientific.net/AMM.461.213>
- [2] Rubenson J, Lioyd DG, Heliams DB, Besier TF, Fournier PA. Adaptations for economical bipedal running: the effect of limb structure on three-dimensional joint mechanics. *J R Soc Interface* 2008; 8:740–55; <https://doi.org/10.1098/rsif.2010.0466>
- [3] Baciadonna L, Zucca P, Tommasi L. Posture in ovo as a precursor of footedness in ostriches (*Struthio Camelus*). *Behav Process* 2009; 83:130–3; <https://doi.org/10.1016/j.beproc.2009.09.004>
- [4] Schaller NU, D'août K, Villa R, Herkner B, Aerts P. Toe function and dynamic pressure distribution in ostrich locomotion. *J Exp Biol* 2011; 214:1123–30; <https://doi.org/10.1242/jeb.043596>
- [5] Ottani V, Raspanti M, Ruggeri A. Collagen structure and functional implications. *Micron* 2001; 32:251–60; [https://doi.org/10.1016/S0968-4328\(00\)00042-1](https://doi.org/10.1016/S0968-4328(00)00042-1)
- [6] Magnusson SP, Hansen P, Kjaer M. Tendon properties in relation to muscular activity and physical training. *Scand J Med Sci Spor* 2003; 13:211–23; <https://doi.org/10.1034/j.1600-0838.2003.00308.x>
- [7] karakurum G, Güleç A, Büyükbeceli O, Karadağ E. The ostrich: an excellent tendon source for the biomechanical studies. *Gülhane Tip Dergisi* 2003; 45(2):180–1.
- [8] Rawson S, Cartmell S, Wong J. Suture techniques for tendon repair; a comparative review. *Muscles Ligaments Tendons J* 2013; 3(3):220–8; doi: 10.11138/mltj/2013.3.3.220
- [9] Rudge WBJ, James M. Flexor tendon injuries in the hand: a UK survey of repair techniques and suture materials—are we following the evidence? *Int Scholarly Res Notices* 2014; 2014:1–4; <https://doi.org/10.1155/2014/687128>
- [10] Smith RKW. Tendon and ligament injury. *AAEP PROCEEDINGS* 2008; 54:475–501.
- [11] Bezuidenhout AJ. Anatomy. In: Deeming DC (ed.). *The ostrich – biology, production and health*, University Press, Cambridge, UK, pp 13–49, 1999.
- [12] Abourachid A, Renous S. Bipedal locomotion in ratites (Paleognathiform): examples of cursorial birds. *Ibis* 2000; 142:538–49; <https://doi.org/10.1111/j.1474-919X.2000.tb04455.x>
- [13] Weissengruber GE, Gangl D, Forstenpointner G, Probst A. Morphological features of the patellae of the ostrich (*Struthio camelus* Linné 1758). *Proceedings of the XXIV Congress of the European Association of Veterinary Anatomists*, Brno, Czech Republic, pp 66, 2002.
- [14] Gangl D, Weissengruber GE, Egerbacher M, Forstenpointner G. Anatomical description of the muscles of the pelvic limb in the ostrich (*Struthio camelus*). *Anat Histol Embryol J Vet Med Series C* 2004; 33(2):100–14; <https://doi.org/10.1111/j.1439-0264.2003.00522.x>
- [15] Schaller NU, Herkner B, Prinzing R. Locomotor characteristics of the ostrich (*Struthio camelus*). I: morphometric and morphological analyses. *Proceedings of the 3rd International Ratite Science Symposium*, Madrid, Spain, pp 83–90, 2005.
- [16] Zhang R, Wang H, Zeng G, Zhou C, Pan R, Wang Q, Li J. Anatomical study of the ostrich (*Struthio camelus*) foot locomotor system. *Indian J Anim Res* 2016; 50(4):476–83; <https://doi.org/10.18805/ijar.9300>
- [17] Zhang R, Wang H, Zeng G, Li J. Finite element modeling and analysis in locomotion system of ostrich (*Struthio camelus*) foot. *Biomed Res* 2016; 27(4):1416–22.
- [18] Daley MA, Birn-Jeffery A. Scaling of avian bipedal locomotion reveals independent effects of body mass and leg posture on gait. *J Exp Biol* 2018; 221:1–13; <https://doi.org/10.1242/jeb.152538>
- [19] Van den Berge JC, Zweers GA. Myologia. In: Baumel, JJ, King AS, Breazile JE, Evans HE, van den Berge JC (ed.). *Handbook of avian anatomy: nomina anatomica avium*. 2nd edition, Publications of Nuttall Ornithological Club, Cambridge, MA, pp 189–247, 1993.
- [20] Weissengruber GE, Forstenpointner G, Gangl D. Gut zu Fuß—funktionell-anatomische Aspekte des bipeden Laufens beim Afrikanischen Strauß (*Struthio camelus* Linné, 1758). *Wien Tierärztl Mschr* 2003; 90:67–78.
- [21] Liswaniso D. A morphological and diagnostic imaging study of the distal pelvic limb of the ostrich (*Struthio camelus*). MSc Thesis in University of Glasgow, Scotland, UK, 1996. Available via <https://doi.org/10.4314/jost.v1i1.17509>

- [22] Quinn TH, Baumel JJ. The digital tendon locking mechanism of the avian foot (Aves). *Zoomorphology* 1990; 109:281–93; <https://doi.org/10.1002/jez.1714>
- [23] Pavaux C, Lignereux Y. Une dissection myologique de la Jambe et du Pied de l'Atruche (*Struthio camelus*). *Anat Histol Embryol* 1995; 24:127–31; <https://doi.org/10.1111/j.1439-0264.1995.tb00023.x>
- [24] Zhang R, Han D, Luo G, Ling L, Li G, Ji Q, et al. Macroscopic and microscopic analyses in flexor tendons of the tarsometatarso-phalangeal joint of ostrich (*Struthio camelus*) foot with energy storage and shock absorption. *J Morphol* 2018; 279:302–11; <https://doi.org/10.1002/jmor.20772>
- [25] Smith NC, Wilson AM, Jespers KJ, Payne RC. Muscle architecture and functional anatomy of the pelvic limb of the ostrich (*Struthio camelus*). *J Anat* 2006; 209:765–79; <https://doi.org/10.1111/j.1469-7580.2006.00658.x>
- [26] Soroori S, Masoudifard M, Vajhi AR, Rostami A, Salimi M. Ultrasonography study of tendons and ligaments of metacarpal region in the camel (*Camelus dromedaries*). *Iranian J Vet Med* 2011; 5:85–8; <https://doi.org/10.22059/ijvm.2011.23102>